https://dx.doi.org/10.1016/j.scitotenv.2022.154774

Ambient acidic ultrafine particles in different land-use areas in two representative Chinese cities

Haoxian Lu[1], Gehui Wang[2], Hai Guo[1]*

1. Air Quality Studies, Department of Civil and Environmental Engineering, The Hong Kong Polytechnic University, Hong Kong, China
2. School of Geographic Sciences, East China Normal University, Shanghai, China

Abstract

The adverse effects of acidic ultrafine particles (AUFPs) have been widely recognized in scientific communities. However, a handful of studies successfully acquired the concentrations of AUFPs in the atmosphere. To explore the AUFPs pollution, six extensive measurements were for the first time conducted in the roadside, urban and rural areas in Hong Kong, and the urban area in Shanghai between 2017 and 2020. The concentrations of AUFPs and UFPs, and the proportions of AUFPs in UFPs were obtained. The concentration of UFPs was the highest at the roadside site, followed by the urban site and the rural site, while the proportion of AUFPs in UFPs showed a contrary trend. The difference, on one hand, indicated the potential transformation of AUFPs from non-acidic UFPs during the transport and aging of air masses, and on the other hand, suggested the minor contribution of anthropogenic sources to the emission of AUFPs. In addition, the urban area in Hong Kong suffered from heavier pollution of UFPs and AUFPs than that in Shanghai. As for size distribution, the proportion of AUFPs in UFPs peaked in the size range of 35-50 nm and 50-75 nm in roadside and urban area, respectively. In rural area, the peak was observed in the size range of 5-10 nm, which might indicate the stimulation of new particle formation with the AUFPs as seeds. Furthermore, in the urban areas of Hong Kong and Shanghai, no significant difference was found for the geometric mean diameters of UFPs and AUFPs ($p > 0.05$). At last, the sulfuric acid proxy was positively correlated with the proportions of AUFPs in UFPs but not well correlated with the AUFPs levels. The results suggested the important roles of interaction between sulfuric acid vapor and non-acidic UFPs in AUFPs formation. Due to the significant reduction of sulfur dioxide in China during the last decade, the pollution of AUFPs in urban areas was alleviated.

Key words: Acidic Ultrafine Particles (AUFPs); Field measurements; Diffusion Sampler (DS);

29 Atomic Force Microscope.

30 1. Introduction

31 Aerosol is defined as airborne particles, which contain more than 90% ultrafine particles (UFPs, i.e.,
32 aerodynamic diameter <100nm) in terms of number concentration (Karottki et al., 2015; Rim et al.,
33 2016). It is believed that UFPs are able to carry the greatest amount of inflammation per unit PM mass
34 because of high particle number (PN), high lung deposition efficiency and large surface area, compared
35 to fine and coarse particles (Wang et al., 2012). However, components of UFPs are not equally
36 detrimental (Utell et al., 1982; Schlesinger, 1989; McGranahan and Murray, 2012). Among all the
37 chemical components in ambient UFPs, sulfuric acid (H_2SO_4) and ammonium bisulfate (NH_4HSO_4)
38 are the significant and harmful chemicals, forming acidic ultrafine particles (AUFPs). AUFPs have
39 been proved to be closely associated with total mortality, morbidity and hospital admissions for
40 respiratory diseases (*e.g.*, Thurston et al., 1989, 1992, 1994; Lippmann and Thurston, 1996; Peters et
41 al., 1997; Wichmann et al., 2000; Cohen et al., 2000; Lu et al., 2020). Specifically, the respiratory
42 diseases include the prevalence of bronchitis and lung function decrements. In addition to health effect,
43 AUFPs are closely related to new particle formation (NPF) as AUFPs can facilitate the particle
44 formation and growth (Guo et al., 2012; Wang et al., 2014a). However, the relationships of AUFPs
45 with NPF and particle growth were only evidenced by the concentrations of sulfuric acid vapor and/or
46 *pH* of particles in the NPF events in previous studies, rather than the concentration of AUFPs (Riipinen
47 et al., 2007; Sipilä et al., 2010). Thus, it is crucial to collect sufficient data of AUFPs in the atmosphere
48 to better understand the association of AUFPs with health impact and the direct connection of NPF
49 with AUFPs.

50 A handful of studies successfully measured AUFPs in the atmosphere. In 1990s, Cohen et al. (2000,
51 2004a) firstly applied an iron nanofilm detector to measure the AUFPs in downtown New York, but
52 no acidic particles were detected due to insufficient sampling duration. Later, Cohen et al. (2004b)
53 reported AUFPs levels of 100-1800 /cm^3 in Tuxedo town of New York state after a longer sampling
54 duration. More than 10 years later, Wang et al. (2012) successfully observed and quantified the AUFPs
55 at a mountain site of Hong Kong by collecting airborne UFPs onto a nanofilm detector mounted in an
56 electrostatic precipitator (ESP) and then scanning the detector using an Atomic Force Microscope

(AFM). They found that the daily average concentration of AUFPs was ~ 2 × 10^3 /cm^3, which accounted for ~30% of total UFPs. Further, to overcome the shortage of the previous method, Wang et al. (2014b) applied their own developed diffusion sampler (DS) together with the same nanofilm detectors to measure UFPs and AUFPs at an urban site in Hong Kong. The daily average concentrations of AUFPs and UFPs were ~ 9 × 10^3 /cm^3 and ~ 2 × 10^4 /cm^3, respectively. These limited studies clearly showed that the measurements of ambient AUFPs are far from enough, not to mention the inconsistent methods used in these previous studies. As such, the abundance, size distribution, and spatiotemporal characteristics of AUFPs in the atmosphere are poorly understood.

To fill the gap, in the study, AUFPs were extensively measured in different land-use areas in different Chinese cities using the method developed by Wang et al. (2014b) (*i.e.*, DS + AFM). Three types of land-use areas were chosen to conduct the samplings, including urban, roadside and rural areas. In general, particulate pollution in urban and roadside areas is mainly influenced by anthropogenic emissions, while in rural area it is mostly affected by biogenic emissions and regional transport. Therefore, in urban and roadside areas, the number concentration of UFPs could be high due to strong source emissions and AUFPs could be abundant if sulfur content in the fuel/oil is high. Moreover, the values of UFPs and AUFPs in rural areas could indicate the background level of particulate pollution and the formation mechanism of AUFPs in natural environment and during regional transport. Specifically, two field measurements were carried out at an urban site (one on 6 January-17 February 2017 and another on 15 - 25 April 2019) and at a roadside site (23 November-14 December 2017 and 10 -17 July 2019, respectively) in Hong Kong, while another sampling campaign was conducted in a rural area of Hong Kong from 2 November to 23 November 2020 to understand the spatiotemporal variations of AUFPs pollution in Hong Kong. In addition, to investigate the difference of AUFPs pollution in different cities, a sampling campaign was undertaken in Shanghai on 11 - 29 September 2019. Shanghai was specifically chosen for inter-comparison of AUFPs pollution because of its distinct geographical feature, meteorological conditions, anthropogenic emissions, and urban infrastructures. This is the first comprehensive attempt to unravel the concentrations, size distributions and spatiotemporal variations of AUFPs. Obtainment of the concentration of AUFPs is the basic and

prerequisite information to conduct health risk assessment of AUFPs pollution. The findings are expected to enhance our understanding of AUFPs in the atmosphere, help establish a database of AUFPs and provide additional references for AUFPs control guideline and future air quality research.

2. Methodology

2.1 DS+AFM system

The concentrations of UFPs and AUPFs were measured using the DS+AFM method in the study, developed by Wang et al. (2014b). In brief, the UFPs and AUFPs were deposited on the surface of metallic nano-film detectors, which were placed in the DS. After collection, the UFPs and AUFPs were visualized, identified and counted using the AFM. By considering the collection efficiency, sampling period and sample flow, the number concentrations of UFPs and AUFPs in the atmosphere were ascertained. More details of the method can be found in the previous study (Wang et al., 2014b).

2.1.1 Structure of the diffusion sampler (DS)

The DS was originally developed in our previous study to measure AUFPs in the atmosphere (Wang et al., 2014b). The DS was made of stainless steel with a flat and rectangular channel with 1.0 mm height, 50 mm width, and 500 mm length. The size of the DS inlet was 1×50 mm (height × width). The DS had nine circular sampling spots to place the metal-silicon detectors (diameter × height: 7× 0.4 mm) comprising three groups (Wang et al., 2014b; Fig. 1). The locations of the three sampling spots were at 7.0, 201.5, and 472.5 mm (midpoint of the circular recess) from the inlet along the length of the channel, respectively. The L1~L2, L3~L4, and L5~L6 were the distances of left and right sides of metal-silicon detectors from the inlet at the three locations, respectively. Air was drawn through the DS by a low-flow pump (0.05 L/min). Air leakage was avoided by sealing the channel with a layer of rubber. The detectors collected by the DS were topographically analyzed by the AFM (NanoScope, Multi-mode 8, Veeco Instrument Inc., USA) to identify and enumerate the acidic and non-acidic particles and obtain the sizes of particles. In a field measurement, the sampling durations were 2-4 days, depending on the concentrations of atmospheric particles.

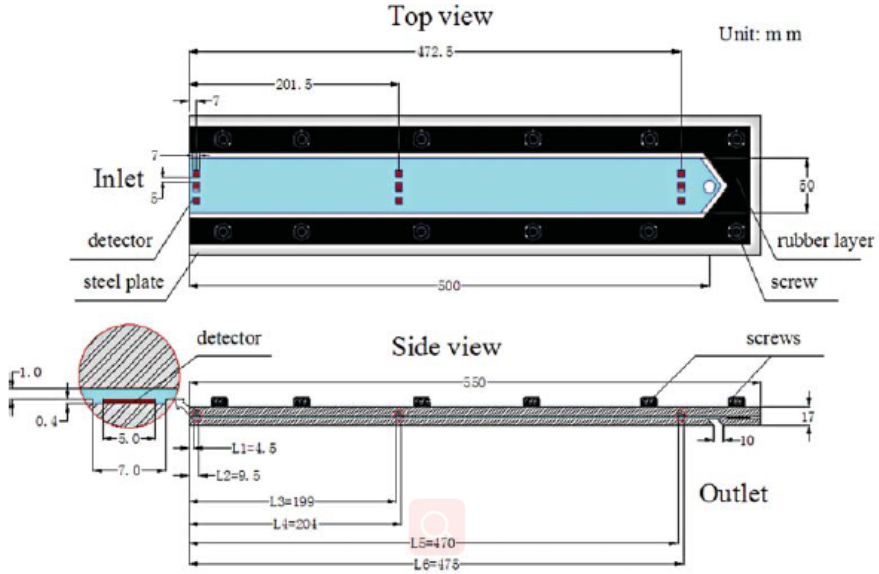

Fig. 1 Schematic diagram of the DS (Wang et al., 2014b).

2.1.2 Collection efficiency of DS

The collection efficiencies of the DS at each spot were calibrated and ascertained in the previous study (Eqs. 1, 2, 3, 4 and 5; Wang et al., 2014b).

$$\Delta\eta_a = 3.20 \times \mu_{L2}\text{^}0.576 - \mu_{L1}\text{^}0.576 \quad \text{Eq. 1}$$

$$\Delta\eta_b = 1.844 \times [\exp(-8.04\mu_{L3}) - \exp(-8.04 \times \mu_{L4})] \quad \text{Eq. 2}$$

$$\Delta\eta_c = 1.957 \times [\exp(-7.43\mu_{L5}) - \exp(-7.43 \times \mu_{L6})] \quad \text{Eq. 3}$$

$$\mu_{Li} = (D \times L_i \times W)/(Q \times h) \quad \text{Eq. 4}$$

$$D = (k \times T \times Cc \times 10\text{^}10)/(3\pi \times \gamma \times dp) \quad \text{Eq. 5}$$

where $\Delta\eta_a$, $\Delta\eta_b$, and $\Delta\eta_c$ are the collection efficiencies at the sampling spots A, B and C, respectively, μ is deposition parameter, L is channel length (cm), W is channel width (cm), Q is flow rate (cm^3/sec), and h is channel height (cm); D is the diffusion coefficient of the particle (cm^2/sec), k is Boltzmann's constant (1.38×10^{23}), T is the absolute temperature, C_c is the slip correction factor, γ is the air viscosity (1.79×10^{-5} Pa·sec), and d_p is the particle diameter (μm). As such, the collection efficiency of particles with different sizes at each spot at the flow rate of 0.05 L/min is calculated and plotted (Fig. 2).

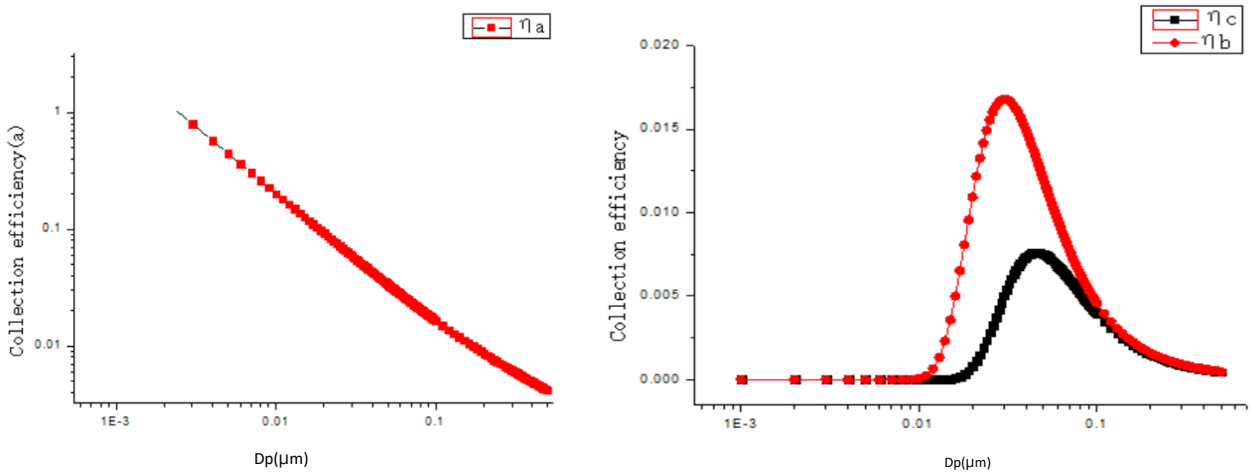

Fig. 2 The stepwise particle collection efficiency of the three sampling spots in the DS.

Thus, the particle concentrations in the atmosphere, derived from the number of deposited particles on the detectors scanned by the AFM, are given as follows (Eq. 6).

$$\text{Concentration}=(2.5\times10^{7})/A\times\Sigma\{N_{dpi}/(\eta_i\times Q\times t)\} \quad \text{Eq. 6}$$

where 2.5×10^{7} is the area of the metal-silicon detector (5mm × 5mm = 2.5×10^{7} μm^2); A is the scanned area on the detector by AFM (μm^2); N_{dpi} is the counted number of particles in the i^{th} size bin; η_i is the deposition efficiency of the particles in the same size bin; and t is the sampling time (sec.). By summing up the calculated number concentration in each size bin, the average number concentrations of particles were obtained.

2.2 Sampling sites and sampling periods

In this study, AUFPs were measured using the DS+AFM method at different sites in Hong Kong and Shanghai from 2017 to 2020 through six sampling campaigns. Field measurements were conducted in three land-use areas in Hong Kong, including an urban site, a roadside site and a rural site. At the urban site, two campaigns were carried out from 6 January to 17 February 2017 and from 11 April to 25 April 2019 (Fig. 3). At the roadside site, two measurements were also conducted from 23 November to 14 December 2017 and from 10 July to 17 July 2019 (Fig. 3). The samplings in urban and roadside areas aimed to explore the seasonal variations of AUFPs pollution (cool season vs. warm season). The one at the rural site (Hok Tsui) was performed from 2 November to 23 November 2020 (Fig. 4). Outside Hong Kong, the sampling in Shanghai was implemented at an urban site from 11 September to 29

September 2019 (Fig. 5). Only one sampling was conducted in the rural area in Hong Kong and the urban area in Shanghai due to limited manpower and measurement device. In this study, the measurements above were marked as samplings I, II, III, IV, V and VI, for 2017 Hong Kong roadside sampling, 2017 Hong Kong urban sampling, 2019 Hong Kong roadside sampling, 2019 Hong Kong urban sampling, 2020 Hong Kong rural sampling and 2019 Shanghai urban sampling, respectively. The urban site (22.303°N, 114.180°E) in Hong Kong is on the rooftop of a building in the campus of Hong Kong Polytechnic University at Hung Hom, Kowloon (Z Core). This site is significantly affected by the anthropogenic emissions as it is located near main roads and surrounded by residential areas (Fig. S1). The roadside site (22.306°N, 114.179°E) is near the cross-harbour tunnel (CHT), which is one of the busiest roads in Hong Kong. Traffic emission is the primary source at the roadside site (Fig. S1).

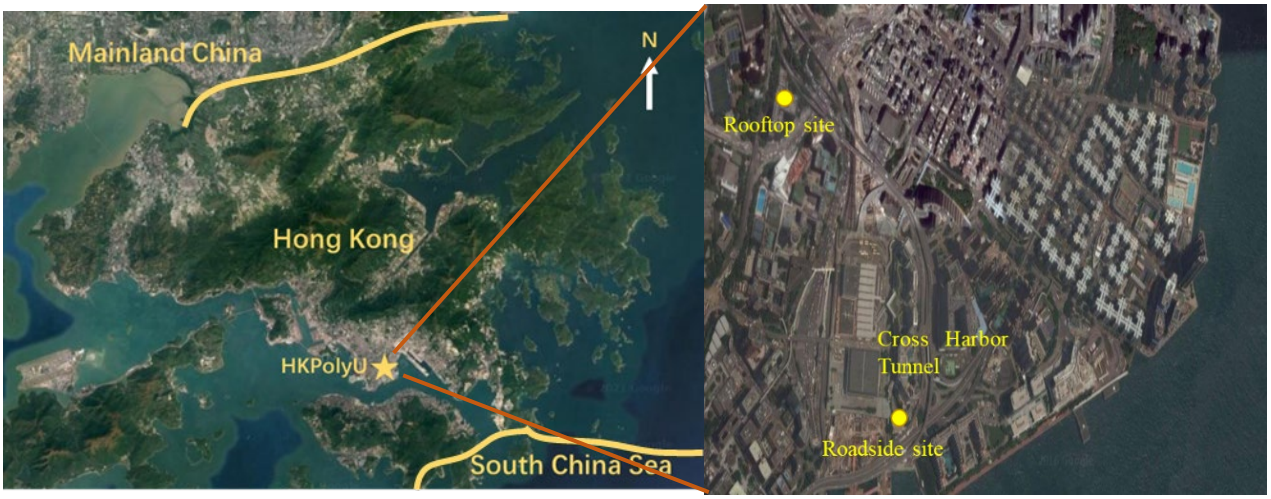

Fig. 3 Geographical location of the urban and roadside sites in Hong Kong

The rural site of Hong Kong is in Hok Tsui (HT). The HT site (22.209°N, 114.253°E) is a relatively remote coastal site, located at the southeastern tip of Hong Kong. A country park locates 2 km to the north of the sampling site, and there are many broad-leaved trees within 500 m of the site (Fig S2). The site has long been regarded as a regionally urban background site in South China, given that air pollutants in the adjoining Pearl River Delta reach the site within a few hours (Zhang et al., 2012).

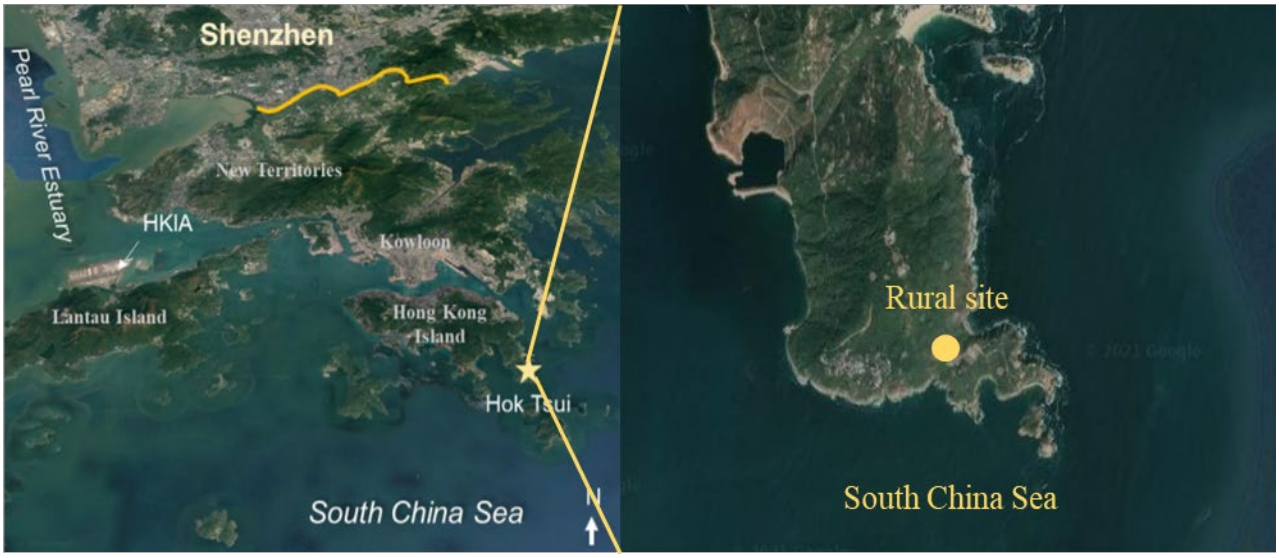

Fig. 4 Geographical location of the rural site in Hong Kong

The urban site in Shanghai is in the East China Normal University (Minhang Campus) (31.228°N, 121.407°E). Sampler was put on the top of a container located in a playground of the university (Fig. S3). The site is located in the south of downtown Shanghai, where residential activities and vehicle emissions are the main sources of air pollutants.

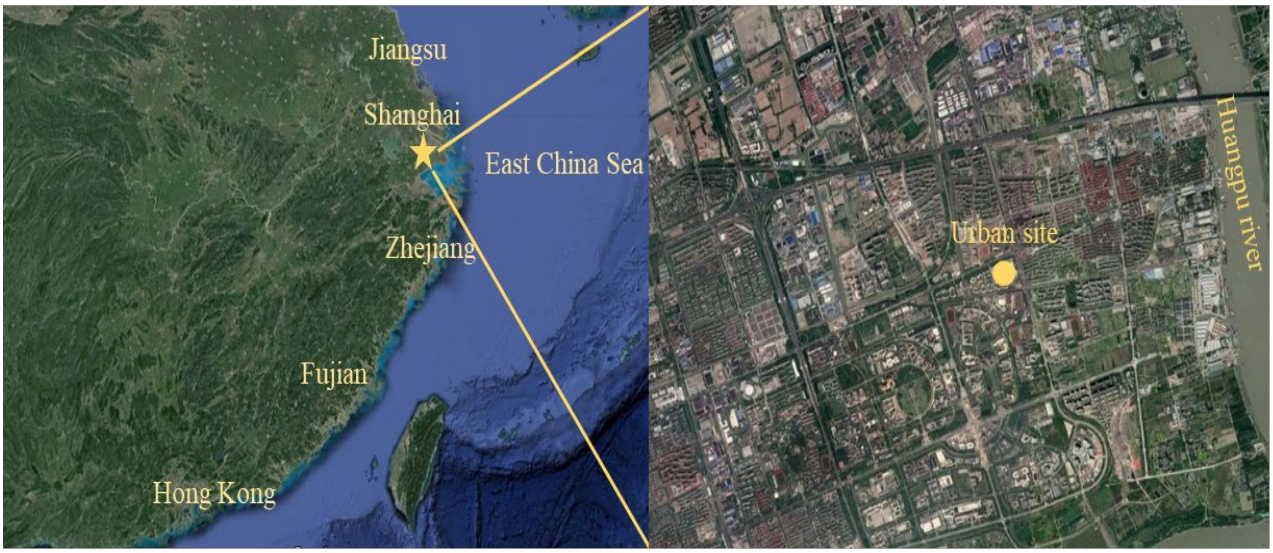

Fig. 5 Geographical location of the urban site in Shanghai

2.3 Concentration of sulfuric acid (SA) vapor

To investigate the relationship of sulfuric acid vapor (Q_{sa}) with AUFPs, a predictive proxy based on solar radiation, SO_2 concentration, condensation sink (CS) and relative humidity was used to estimate

sulfuric acid concentration (Mikkonen et al., 2011; Eq. 7). The CS, presented as the loss rate of molecules onto existing particles, was calculated based on the particle size distribution. In the study, the SO_2 data for Q_{sa} estimation in Hong Kong were obtained from Hong Kong Environmental Protection Department (HKEPD) (https://cd.epic.epd.gov.hk/EPICDI/air/station /?lang=zh), while in Shanghai they were collected from China National Environmental Monitoring Center (http://106.37.208.233:20035/). Meteorological data in Hong Kong and Shanghai were acquired from Hong Kong Observatory (https://www.hko.gov.hk/tc/) and the fifth generation European Centre for Medium-Range Weather Forecasts reanalysis data (https://www.ecmwf.int/), respectively. The average atmospheric conditions used to calculate the Q_{sa} in different samplings are listed in Table S1. The equations for calculating Q_{sa} and CS are shown in Eq. 7 and Eq. 8.

$$Q_{sa}= 8.21\times10^{-3} \cdot k \cdot [SO_2]^{0.62} \cdot [SR] \cdot (CS \cdot RH)^{-0.13} \quad \text{Eq. 7}$$

where k is a constant value 1.035, SO_2 is the measured concentration in ppb, SR is the solar radiation in W/m^2, RH is the relative humidity in % and CS is the condensation sink in s^{-1}.

$$CS = 2\pi d\int D_p \cdot \beta_M(D_p)N(D_p)dD_p = 2\pi d\sum \beta_{Mi}D_{pi}N_i \quad \text{Eq. 8}$$

where d is the diffusion coefficient of the condensing vapor, β_{Mi} is the transitional regime correction factor in size bin *i*, D_{pi} is the average particle diameter in size bin *i*, and N_i is the particle number concentration in the corresponding size bin.

3. Results and discussion

3.1 Concentrations of UFPs and AUFPs

Fig. 6 presents the concentrations of AUFPs and UFPs in different land-use areas and cities together with the proportions of AUFPs in UFPs. The concentrations of UFPs (mean ± standard deviation (SD)) were $(1.48 \pm 0.64) \times10^4$, $(1.39 \pm 0.65) \times10^4$, $(1.71 \pm 0.92) \times10^4$, $(1.57 \pm 0.84) \times10^4$, $(0.60 \pm 0.20) \times10^4$ and $(1.21 \pm 0.49) \times10^4$ $/cm^3$ for sampling I (2017 Hong Kong roadside), II (2017 Hong Kong urban), III (2019 Hong Kong roadside), IV (2019 Hong Kong urban sampling), V (2020 Hong Kong rural sampling) and VI (2019 Shanghai urban sampling), respectively. In comparison, the concentrations of UFPs were the lowest in the rural area in Hong Kong ($p < 0.05$) due to sparse anthropogenic emissions. The levels of UFPs at the roadside site were slightly higher than those at the urban site because the

roadside site was closer to emission sources, *i.e.*, motor vehicles which directly emit abundant UFPs (Zhai et al., 2016; Campagnolo et al., 2019). Nevertheless, the difference was not significant ($p > 0.05$). In addition, despite different years and seasons when the measurements were conducted at the roadside site or the urban site, no significant differences in the concentrations of UFPs were found (both $p > 0.05$), suggesting the pollution associated with UFPs was relatively stable in both urban and roadside areas of Hong Kong in these years and in different seasons. Noteworthily, the concentration of UFPs in urban area of Shanghai was lower than that in urban area of Hong Kong ($p < 0.05$), probably implying less pollution of UFPs in urban Shanghai. However, it is worth noting that the sampling in Shanghai was conducted in the plum rainy season, which might also lead to the low concentrations of UFPs. Compared to the UFPs levels in the world, the UFPs level in China was higher than that in Japan (Yoshino et.al., 2021), Korea (Park et al., 2008), Europe and USA (De Jesus et al., 2019).

For AUFPs, the concentration was $(0.31 \pm 0.18) \times 10^4$, $(0.37 \pm 0.30) \times 10^4$, $(0.37 \pm 0.26) \times 10^4$, $(0.42 \pm 0.28) \times 10^4$, $(0.22 \pm 0.10) \times 10^4$ and $(0.27 \pm 0.19) \times 10^4$ /cm^3 for sampling I, II, III, IV, V and VI, respectively. Clearly, the concentration of AUFPs was the lowest in rural area ($p < 0.05$). No significant spatial and temporal differences were found in the concentration of AUFPs between the urban site and the roadside site in Hong Kong between 2017 and 2019 (all $p > 0.05$), consistent with the stable level of UFPs pollution in both urban and roadside areas. Similar to UFPs, the concentration of AUFPs in urban area of Shanghai was lower than that in urban Hong Kong ($p < 0.05$).

The AUFPs concentration accounted for the highest proportion of UFPs concentration in rural area (*i.e.*, 36%) (Fig. 6), followed by that in urban areas (*i.e.*, sampling II: 27%, sampling IV: 26% and sampling VI: 23%) and in roadside areas (*i.e.*, sampling I: 20% and sampling III: 21%). The proportion of AUFPs in UFPs had inverse correlation with the distance to the emission sources, implying that the AUFPs emitted from anthropogenic sources was minor and the AUFPs might be potentially transformed from non-acidic UFPs by heterogeneous reaction of acidic vapors with preexisting non-acidic particles and/or condensation of acidic vapor on the surface of non-acidic particles during the transport and aging of air masses. Nevertheless, it must be admitted that the field measurements in the study were basically short-term, which may exist some uncertainties for the above comparisons since

the ambient particulates vary with the atmospheric conditions as well as the source emission profiles. Therefore, it is strongly suggested that prolonged and more samplings be conducted in future study.

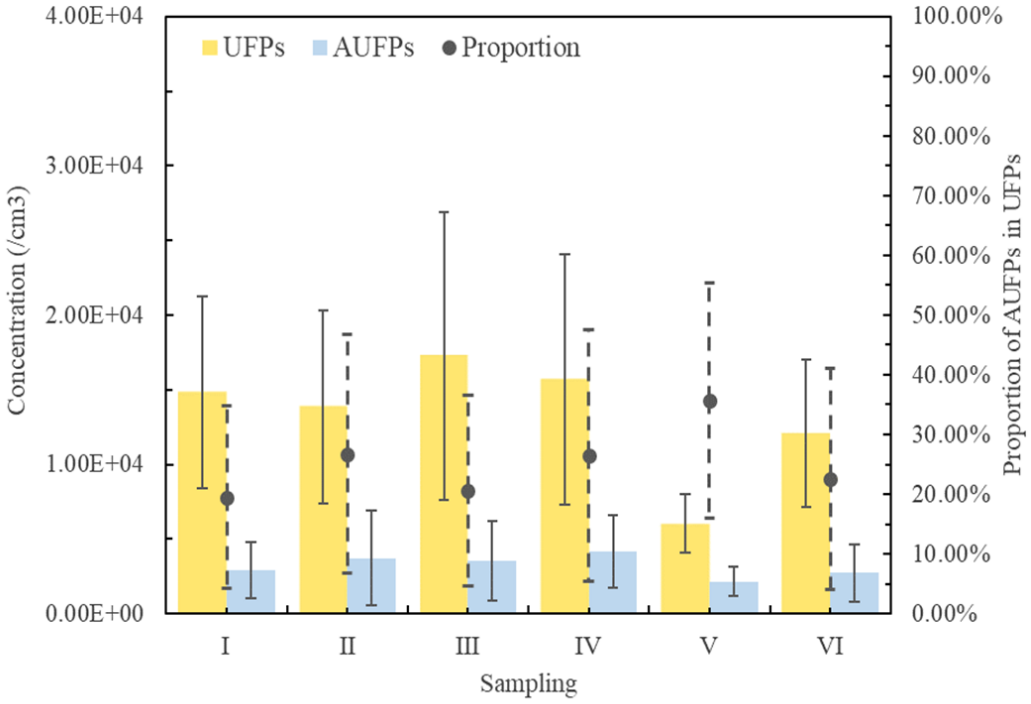

Fig. 6 Concentrations of UFPs and AUFPs, and proportion of AUFPs in UFPs in different land-use areas and cities

3.2 Size distributions of UFPs and AUFPs

Fig. 7 shows the size distributions of AUFPs and UFPs in different land-use areas and cities, as well as the proportions of AUFPs in UFPs in different size bins. Eight size bins were categorized for particles with sizes from 5 nm to 200 nm (*i.e.*, 5-10 nm, 10-20 nm, 20-35 nm, 35-50 nm, 50-70 nm, 70-100 nm, 100-150 nm and 150-200 nm). The geometric mean diameter (GMD) of the size distribution was calculated using the following equation (Eq. 9):

$$GMD = \Sigma N_i \bullet d_{pi} / N \quad \text{Eq. 9}$$

where N_i is the particle number concentration in i_{th} size bin, d_{pi} is the average particle diameter (nm) in i_{th} size bin, and N is the total particle number concentration of all size bins.

The size distributions of UFPs were normal in all the six sampling campaigns. Concentration of UFPs generally peaked in the size range of 20-35 nm or 35-50 nm, in line with the results of previous studies (Li et al., 2007; Cheng et al., 2012). The nucleation-mode and Aitken-mode particles (<100 nm)

253 dominated the UFPs concentration, accounting for ~90% of the total particle number concentration.
254 The GMD of UFPs was 28.0 nm, 35.8 nm, 33.6 nm, 34.5 nm, 38.1 nm and 35.4 nm in samplings I, II,
255 III, IV, V and VI, respectively. The highest GMD value was found in rural area (*i.e.*, 38.1 nm), while
256 the GMD values in urban areas (34.5 – 35.8 nm) were similar to those in roadside areas (28.0 – 33.6
257 nm). The GMD values were generally associated with the age of air masses in different land-use areas.
258 The transport of pollutants from an urban area to a rural area provided enough time for particles to
259 coagulate and grow up and thus increased the GMD (Yao et al., 2010; Šmejkalová et al., 2020).
260 Similarly, the size distributions of AUFPs were normal with peaks at 20-35 nm or 35-50 nm. The
261 GMDs of AUFPs were 28.7 nm, 34.3 nm, 36.1 nm, 36.0 nm, 32.8 nm and 34.3 nm for samplings I, II,
262 III, IV, V and VI, respectively, analogous to the corresponding GMDs of UFPs ($p > 0.05$). Further,
263 over 90% of AUFPs composed of particles in nucleation and Aitken modes. Few AUFPs were in the
264 size range of 150-200 nm, consistent with the results of previous studies, which found that sulfuric
265 acid and/or nitric acid are usually present in UFPs at the initial formation stage to promote particle
266 formation and growth (Schlesinger and Cassee, 2003; Wang et al., 2020). In addition, no significant
267 difference in GMDs of AUFPs and UFPs was found in urban areas between Hong Kong and Shanghai
268 ($p > 0.05$), perhaps suggesting similar emission sources and/or chemical formation mechanisms of
269 UFPs and AUFPs in these two cities.
270 The proportion of AUFPs in UFPs showed distinct patterns in different land-use areas. In roadside
271 areas, the proportion peaked at 35-50 nm, while the maximum proportion in urban areas was in the
272 size range of 50-75 nm. The hysteretic peak in urban areas might indicate the aggregation of AUFPs
273 with non-acidic UFPs during the transport from source areas to receptor areas. However, the highest
274 proportion in rural area was observed in the range of 5-10 nm. The high proportion of AUFPs in UFPs
275 in small size range in rural area might suggest the stimulation of new particle formation (NPF) with
276 the AUFPs as seeds that were not easy to be aggregated by other low-concentration preexisting
277 particles in a relatively clean environment. In addition, anthropogenic sources are scarce in rural area,
278 especially for vehicle emissions. Automobile exhaust is an important source of particles smaller than
279 20 nm (Mathis et al., 2004; Casati et al., 2007). Hence, a large amount of automobile exhaust emissions

in urban and roadside areas resulted in a lower proportion of AUFPs in UFPs in the small size range than in rural areas.

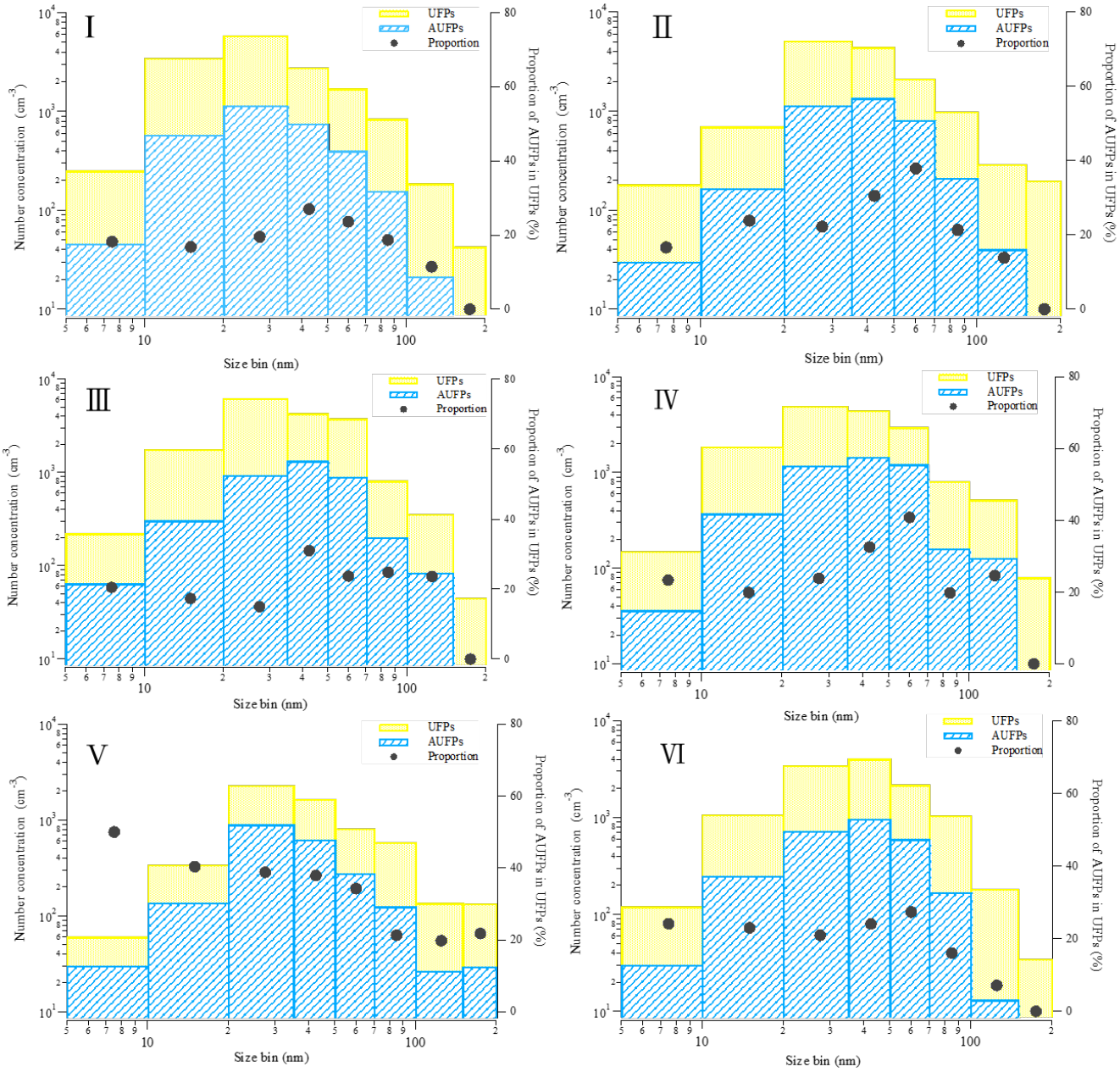

Fig. 7 Size distributions of UFPs and AUFPs with the proportions of AUFPs in UFPs in different size bins in different land-use areas and cities.

3.3 Correlation of estimated sulfuric acid vapor with AUFPs

Sulfuric acid vapor has been proved to be related to NPF (Kulmala et al., 2000; Guo et al., 2012; Wang et al., 2014a). Thus, it is expected that some of these newly-formed particles are acidic. Fig. 8 illustrates

the correlation between proportion of AUFPs in UFPs and Q_{sa} at different concentrations of AUFPs in field measurements. It is noteworthy that the AUFPs data measured in previous studies were also used for comparison purpose (Wang et al., 2012, 2014b). It was found that the proportion of AUFPs in UFPs was positively correlated with the Q_{sa} ($R^2 = 0.71$), while no obvious relationship was observed between the concentration of AUFPs and the Q_{sa} ($R^2 = 0.17$), especially in rural areas. In other words, although the levels of Q_{sa} were high in the rural areas, concentrations of AUFPs were even lower than those in urban and roadside areas. It is well known that condensation of compounds with low vapor pressure such as sulfuric acid and nitric acid on preexisting particles and coagulation of these compounds are important mechanisms to form new particles (Schlesinger and Cassee, 2003; Wang et al., 2020). Both pathways could increase the acidity of particles and lead to the formation of AUFPs if the vapor of those compounds is acidic. Theoretically, a high Q_{sa} level would result in the formation of more AUFPs. However, another factor determining the concentration of AUFPs is also important, namely, the concentration of preexisting particles. If their concentration is higher together with higher Q_{sa} level, more AUFPs will be generated. As such, it is understandable why Q_{sa} does not have positive correlation with the concentration of AUFPs but the proportion of AUFPs in UFPs. In rural areas, although the concentration of Q_{sa} was higher, the concentration of preexisting particles was low, which led to lower AUFPs but higher proportion of AUFPs in UFPs. In comparison, the higher level of preexisting particles in urban and roadside areas was favorable to more AUFPs formation by providing more chances for condensation of sulfuric acid vapor on non-acidic UFPs. However, since the Q_{sa} level in urban/roadside areas was not as high as that in rural area, and the preexisting particles concentration was higher, the proportion of AUFPs in UFPs would be lower. Moreover, the close relationship of Q_{sa} with AUFPs might indicate the minor contribution of other acids such as nitric or organic acids to the AUFPs. Noteworthily, the AUFPs pollution in urban areas in Hong Kong seemed to be alleviated compared to ten years ago in terms of the AUFPs concentration and the proportion of AUFPs in UFPs. Extremely high AUFPs concentration and proportion of AUFPs in UFPs were found at an urban site in 2010 in Hong Kong (*i.e.*, 9.6×10^3 cm^3 and 45%), significantly higher than those measured at the same urban site and roadside site in 2017 and 2019 in this study (all $p < 0.05$). While the meteorological conditions were different in all the measurements, it was still worth mentioning that the significant

reduction in SO_2 in China might play an important role in the alleviation of AUFPs pollution in urban area. The annual SO_2 concentrations in Hong Kong decreased from 12.0 μg/m^3 in 2010 to 4.0 μg/m^3 in 2019, observed at a roadside monitoring station. In the past, the Hong Kong government implemented several measures to cut the SO_2 emission from vehicles. Although low sulfur fuel oil (LSFO) (Euro IV standard) was set as the minimum requirement for vehicle use in April 2002, the statutory standard has been further tightened to Euro V standard since 2010, which could reduce the SO_2 emissions of existing vehicles by 80% (Hedley et al., 2002; Zhang et al., 2010; https://www.info.gov.hk/gia/general/ 201111/09/P201111090187.htm). Moreover, by the end of 2016, about 50,000 old diesel commercial vehicles (older than Euro IV) were phased out. Low emission zones were set up on busy roads such as Central, Causeway Bay and Mong Kok to only allow buses that met Euro IV emission levels or above to run. The above measures also resulted in lower SO_2/Q_{sa} levels in urban/roadside areas than that in rural area in Hong Kong because LSFO was widely and strictly used in vehicles but not in marine vessels and the standard of LSFO usage in marine vessels (maximum sulfur content: 0.05%) was not as tight as that in vehicles (maximum sulfur content: 0.001%) (https://www.epd.gov.hk/epd/english/environmentinhk/air/air_maincontent.html). Since the rural site was located in a coastal area, it would suffer from more emission of marine vessels and had the higher SO_2/Q_{sa} level. In Shanghai, the SO_2 concentrations sharply decreased from 30 μg/m^3 to 7 μg/m^3 during this decade according to the Shanghai environmental bulletin. On one hand, the mandatory usage of LSFO in vehicles was proposed in 2013 and was completely implemented in mainland China at the end of 2017 (http://www.nea.gov.cn/2013-07/09/c_132525509.htm). On the other hand, the SO_2 emissions from industries and power plants were dramatically reduced in these ten years because of the combustion of low sulfur coal (Wang et al., 2018).

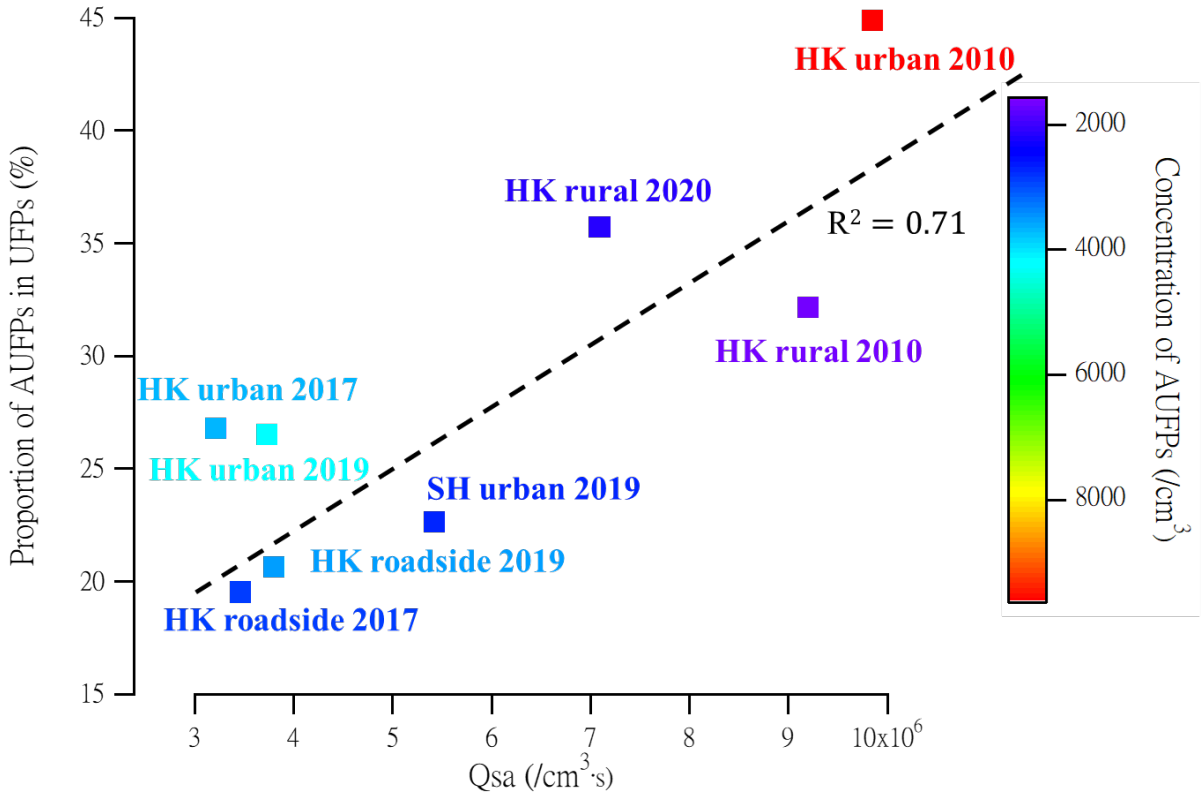

Fig. 8 Correlation of sulfuric acid proxy (Q_{sa}) with proportion of AUFPs in UFPs at different concentrations of AUFPs in different field measurements (HK roadside 2017: sampling I, HK urban 2017: sampling II, HK roadside 2019: sampling III, HK urban 2019: sampling IV, HK rural 2020: sampling V, SH urban 2019: sampling VI, HK rural 2010: Wang et al., 2012 and HK urban 2010: Wang et al., 2014b).

4. Summary

This is the first study to conduct extensive measurements of UFPs and AUFPs in different land-use areas (*i.e.*, roadside, urban and rural) and cities (*i.e.*, Hong Kong and Shanghai) in China. In total, six field measurements were carried out using the DS+AFM method. The results indicated that the concentration of UFPs was the highest at the roadside site, followed by the urban and rural sites. However, an opposite trend was found for the proportion of AUFPs in UFPs. The phenomena suggested the potential transformation of AUFPs from non-acidic UFPs through heterogeneous reaction of acidic vapor with non-acidic UFPs and/or condensation of acidic vapor on the surface of non-acidic UFPs during the transport and aging of air masses and the insignificant emissions of AUFPs

from automobile vehicles. In addition, lower concentrations (mean ± SD) of UFPs ((1.21±0.49) $\times 10^4/cm^3$) and AUFPs ((0.27±0.19) $\times 10^4/cm^3$) were found in urban Shanghai than in Hong Kong ((1.48±0.64) and (0.40±0.27) $\times 10^4/cm^3$, respectively) ($p < 0.05$). Regarding size distribution, the sizes of both UFPs and AUFPs were normally distributed at all sampling sites and the GMDs of both UFPs and AUFPs were from 28 nm to 38 nm. Furthermore, the proportion of AUFPs in UFPs peaked in a larger size range (50-75 nm) in urban areas than that in roadside areas (35-50 nm), suggesting the potential aggregation of AUFPs with non-acidic UFPs during the transport from source areas to receptor areas. In rural area, however, the peak was observed in the smallest size range (*i.e.*, 5-10 nm), indicating the stimulation of NPF with AUFPs as seeds, which were not easily aggregated by other preexisting particles with low concentrations in the relatively clean environment. The GMDs of UFPs and AUFPs in the urban areas between Hong Kong and Shanghai were similar ($p > 0.05$), implying similar emission sources and/or chemical formation mechanisms of UFPs and AUFPs in these two cities. Lastly, the Q_{sa} was positively correlated with the proportion of AUFPs in UFPs (R^2=0.71), while no obvious relationship was found between the Q_{sa} and AUFP levels (R^2=0.17). The results suggested significant formation of AUFPs through heterogeneous reaction of sulfuric acid vapor with non-acidic UFPs and/or condensation of sulfuric acid vapor on non-acidic UFPs at high Q_{sa} level, which led to high proportion of AUFPs in UFPs. However, the AUFPs level might not be high even though the Q_{sa} level was high if the concentration of preexisting particles was low. Compared to the AUFPs pollution in urban Hong Kong ten years ago, the pollution was lowered due to the fact that the concentrations of AUFPs and the proportions of AUFPs in UFPs decreased, possibly due to the successful reduction of SO_2 in China. The reduction in SO_2 in Hong Kong during the last decade was mainly attributed to stricter standards for the use of LSFO and the phase out of old diesel vehicles, while the decrease in SO_2 emissions in Shanghai resulted from the widespread use of LSFO in vehicles nationwide, and the combustion of low sulfur coal in industries and power plants.

Acknowledgements

This study was supported by the Strategic Focus Area scheme of The Research Institute for Sustainable Urban Development at The Hong Kong Polytechnic University (1-BBW9), the University Strategic

Importance scheme at The Hong Kong Polytechnic University (1-ZE1M), the Environment and Conservation Fund (ECF) of the Hong Kong Special Administrative Region (ECF59/2015) and the Hong Kong PhD Fellowship (Project Number: RULW).

CRediT authorship contribution statement

Haoxian Lu: Methodology, Data analysis, Writing – original draft. **Gehui Wang**: Samples collection. **Hai Guo**: Supervision, Resources, Funding acquisition, Writing – review & editing.

Declaration of competing interest

The authors declare that they have no known competing financial interests or personal relationships that could have appeared to influence the work reported in this paper.

References

Campagnolo, D., Cattaneo, A., Corbella, L., Borghi, F., Del Buono, L., Rovelli, S., Spinazzé, A., and Cavallo, D. M. 2019. In-vehicle airborne fine and ultra-fine particulate matter exposure: The impact of leading vehicle emissions. *Environment International*, 123, 407-416.

Casati, R., Scheer, V., Vogt, R., and Benter, T. 2007. Measurement of nucleation and soot mode particle emission from a diesel passenger car in real world and laboratory in situ dilution. *Atmospheric Environment*, *41*(10), 2125-2135.

Cheng, Y., Yu, C. W. F., Huang, Y., Zhang, Y. W., Gao, Y., Yau, P. S., Chan, C. S., and Lee, S. C. 2012. Particle counts and size distributions in the roadside environment. *Indoor and Built Environment*, *21:* 633–641.

Cohen, B. S., Heikkinen, M. S., and Hazi, Y. 2004a. Airborne fine and ultrafine particles near the world trade center disaster site. *Aerosol Science and Technology*, *38*(4), 338-348.

Cohen, B. S., Heikkinen, M. S., Hazi, Y., Guo, H., Peters, P., and Lippmann, M. 2004b. Field evaluation of nanofilm detectors for measuring acidic particles in indoor and outdoor air. *Research report (Health Effects Institute)*, (121), 1-35.

Cohen, B. S., Li, W., Xiong, J. Q., and Lippmann, M. 2000. Detecting H+ in ultrafine ambient aerosol using iron nano-film detectors and scanning probe microscopy. *Applied Occupational and Environmental Hygiene,* 15, 80-89.

De Jesus, A. L., Rahman, M. M., Mazaheri, M., Thompson, H., Knibbs, L. D., Jeong, C., ... and Morawska, L. 2019. Ultrafine particles and PM2. 5 in the air of cities around the world: Are they representative of each other?. *Environment international*, *129*, 118-135.

Guo, H., Wang, D. W., Cheung, K., Ling, Z. H., Chan, C. K., and Yao, X. H. 2012. Observation of aerosol size distribution and new particle formation at a mountain site in subtropical Hong Kong. *Atmospheric Chemistry and Physics*, *12*(20), 9923-9939.

Hedley, A. J., Wong, C. M., Thach, T. Q., Ma, S., Lam, T. H., and Anderson, H. R. 2002. Cardiorespiratory and all-cause mortality after restrictions on sulphur content of fuel in Hong Kong: an intervention study. *The Lancet*, *360*(9346), 1646-1652.

Karottki, D. G., Spilak, M., Frederiksen, M., Jovanovic Andersen, Z., Madsen, A. M., Ketzel, M., and Loft, S. et al., 2015. Indoor and outdoor exposure to ultrafine, fine and microbiologically derived particulate matter related to cardiovascular and respiratory effects in a panel of elderly urban citizens. *International Journal of Environmental Research and Public Health*, *12*(2), 1667-1686.

Kulmala, M., Pirjola, U., and Makela, J. M. 2000. Stable sulphate clusters as a source of new atmospheric particles. *Nature, 404*(6773), 66- 69.

Lu, H., Lyu, X., and Guo, H. 2020. A novel semi-automatic method for measuring acidic ultrafine particles in the atmosphere. *Atmospheric Environment*, 245, 118044.

Li, X., Wang, J., Tu, X. D., Liu, W., and Huang, Z. 2007. Vertical variations of particle number concentration and size distribution in a street canyon in Shanghai, China. *Science of the Total Environment*, *378*(3), 306-316.

Lippmann, M., and Thurston, G. D. 1996. Sulfate concentrations as an indicator of ambient particulate matter air pollution for health risk evaluations. *Journal of Exposure Analysis and Environmental Epidemiology*, *6*(2), 123-146.

Mathis, U., Ristimäki, J., Mohr, M., Keskinen, J., Ntziachristos, L., Samaras, Z., and Mikkanen, P. 2004. Sampling conditions for the measurement of nucleation mode particles in the exhaust of a diesel vehicle. *Aerosol Science and Technology*, *38*(12), 1149-1160.

McGranahan, G., and Murray, F. (Eds.). 2012. *Air pollution and health in rapidly developing countries*. Earthscan.

Mikkonen, S., Korhonen, H., Romakkaniemi, S., Smith, J. N., Joutsensaari, J., Lehtinen, K. E. J., Hamed, A., Breider, T. J., Birmili, W., Spindler, G., Plass-Duelmer, C., Facchini, M. C., and Laaksonen, A. 2011. Meteorological and trace gas factors affecting the number concentration of atmospheric Aitken (D_p=50nm) particles in the continental boundary layer: parameterization using

a multivariate mixed effects model. *Geoscientific Model Development*, *4*(1), 1-13.

Peters, A., Dockery, D. W., Heinrich, J., and Wichmann, H. E. 1997. Short-term effects of particulate air pollution on respiratory morbidity in asthmatic children. *European Respiratory Journal*, 10, 872-879.

Park, K., Park, J. Y., Kwak, J. H., Cho, G. N., and Kim, J. S. 2008. Seasonal and diurnal variations of ultrafine particle concentration in urban Gwangju, Korea: Observation of ultrafine particle events. *Atmospheric Environment*, *42*(4), 788-799.

Riipinen, I., Sihto, S. L., Kulmala, M., Arnold, F., Dal Maso, M., Birmili, W., Saarnio, K., Teinila, K., Kerminen, V. M., Laaksonen, A., and Lehtinen, K. E. J. 2007. Connections between atmospheric sulphuric acid and new particle formation during QUEST IIIIV campaigns in Heidelberg and Hyytiälä. *Atmospheric Chemistry and Physics,* 7, 1899-1914.

Rim, D., Choi, J. I., and Wallace, L. A. 2016. Size-resolved source emission rates of indoor ultrafine particles considering coagulation. *Environmental Science and Technology*, *50*(18), 10031-10038.

Schlesinger, R. B., and Cassee, F. 2003. Atmospheric secondary inorganic particulate matter: the toxicological perspective as a basis for health effects risk assessment. *Inhalation Toxicology*, *15*(3), 197-235.

Sipilä, M., Berndt, T., Petäjä, T., Brus, D., Vanhanen, J., Stratmann, F., Patokoski, J., Roy L. Mauldin III, R., Hyvärinen A.,, Lihavainen, H., and Kulmala, M. 2010. The role of sulfuric acid in atmospheric nucleation. *Science*, *327*(5970), 1243-1246.

Šmejkalová, A. H., Zíková, N., Ždímal, V., Plachá, H., and Bitter, M. 2020. Atmospheric aerosol growth rates at different background station types. *Environmental Science and Pollution Research*, 1-13.

Thurston, G. D., Ito, K., Hayes, C. G., Bates, D. V., and Lippmann, M. 1994. Respiratory hospital admissions and summertime haze air pollution in toronto, ontario: consideration of the role of acid aerosols. *Environmental Research*, 65, 271-290.

Thurston, G. D., Ito, K., Kinney, P. L., and Lippmann, M. 1992. A multi-year study of air pollution and respiratory hospital admissions in three new york state metropolitan areas: results for 1988 and 1989 summers. *Journal of Exposure Analysis and Environmental Epidemiology*, 2, 429-450.

Thurston, G. D., Ito, K., Lippmann, M., and Hayes, C. G. 1989. Re-examination of London mortality in relation to exposure to acidic aerosols during 1962-1973 winters. *Environmental Health Perspectives*, 79, 73-82.

Utell, M. J., Morrow, P. E., and Hyde, R. W. 1982. Comparison of normal and asthmatic

subjects'responses to sulphate pollutant aerosols. In *Inhaled Particles V*, Pergamon, 691-697.

Wang, D. W., Guo, H., and Chan, C. K. 2012. Measuring ambient acidic ultrafine particles using iron nanofilm detectors: method development. *Aerosol Science and Technology,* 46, 521–532.

Wang, D., Guo, H., Cheung, K., and Gan, F. 2014a. Observation of nucleation mode particle burst and new particle formation events at an urban site in Hong Kong. *Atmospheric Environment*, 99, 196-205.

Wang, D. W., Guo, H., and Chan, C. K. 2014b. Diffusion sampler for measurement of acidic ultrafine particles in the atmosphere. *Aerosol Science and Technology*, *48*(12), 1236-1246.

Wang, M., Kong, W., Marten, R., He, X. C., Chen, D., Pfeifer, J., and Donahue, N. M. et al., 2020. Rapid growth of new atmospheric particles by nitric acid and ammonia condensation. *Nature*, *581*(7807), 184-189.

Wang, T., Wang, P., Theys, N., Tong, D., Hendrick, F., Zhang, Q., and Roozendael, M. V. 2018. Spatial and temporal changes in SO_2 regimes over China in the recent decade and the driving mechanism. *Atmospheric Chemistry and Physics*, *18*(24), 18063-18078.

Wichmann, H. E., Spix, C., Tuch, T., Wolke, G., Peters, A., Heinrich, J., Kreyling, W. G., and Heyder, J. 2000. Daily mortality and fine and ultrafine particles in Erfurt, Germany Part I: role of particle number and particle mass. *Research Report (Health Effects Institute)*, (98), 5-86.

Yao, X., Choi, M. Y., Lau, N. T., Lau, A. P., Chan, C. K., and Fang, M. 2010. Growth and shrinkage of new particles in the atmosphere in Hong Kong. *Aerosol Science and Technology*, *44*(8), 639-650.

Yoshino, A., Takami, A., Hara, K., Nishita-Hara, C., Hayashi, M., and Kaneyasu, N. 2021. Contribution of local and transboundary air pollution to the urban air quality of Fukuoka, Japan. *Atmosphere*, *12*(4), 431.

Zhai, W., Wen, D., Xiang, S., Hu, Z., and Noll, K. E. 2016. Ultrafine-particle emission factors as a function of vehicle mode of operation for LDVs based on near-roadway monitoring. *Environmental Science and Technology*, *50*(2), 782-789.

Zhang, K., Hu, J., Gao, S., Liu, Y., Huang, X., and Bao, X. 2010. Sulfur content of gasoline and diesel fuels in northern China. *Energy Policy*, *38*(6), 2934-2940.

Zhang, Y. N., Zhang, Z. S., Chan, C. Y., Engling, G., Sang, X. F., Shi, S., and Wang, X. M. 2012. Levoglucosan and carbonaceous species in the background aerosol of coastal southeast China: case study on transport of biomass burning smoke from the Philippines. *Environmental Science and Pollution Research*, *19*(1), 244-255.